haematologica
Journal of the Ferrata Storti Foundation

The oncogenic ΔNp73 isoform contributes to aggressiveness in acute promyelocytic leukemia

by César Alexander Ortiz Rojas , Diego Antonio Pereira-Martins , Carolina Hassibe Thomé, Germano Aguiar Ferreira, Thiago Mantelo Bianco, Isabel Weinhäuser, Ana Silvia Gouvêa, Priscila S. Scheucher, Cleide Lúcia Araújo Silva, Gerwin Huls, Abel Bermudez, Fernando Garcia, Sharon Pitteri, Vitor Marcel Faça, Emanuele Ammatuna, Jan Jacob Schuringa , Ana Beatriz Glória, Katia Borgia Barbosa Pagnano, Elenaide Coutinho Nunes, Fabiola Traina, Lorena Lôbo de Figueiredo-Pontes and Eduardo Magalhães Rego

Received: September 8, 2025.
Accepted: May 19, 2026.

Citation: César Alexander Ortiz Rojas , Diego Antonio Pereira-Martins , Carolina Hassibe Thomé, Germano Aguiar Ferreira, Thiago Mantelo Bianco, Isabel Weinhäuser, Ana Silvia Gouvêa, Priscila S. Scheucher, Cleide Lúcia Araújo Silva, Gerwin Huls, Abel Bermudez, Fernando Garcia, Sharon Pitteri, Vitor Marcel Faça, Emanuele Ammatuna, Jan Jacob Schuringa , Ana Beatriz Glória, Katia Borgia Barbosa Pagnano, Elenaide Coutinho Nunes, Fabiola Traina, Lorena Lôbo de Figueiredo-Pontes and Eduardo Magalhães Rego. The oncogenic ΔNp73 isoform contributes to aggressiveness in acute promyelocytic leukemia. Haematologica. 2026 May 28. doi: 10.3324/haematol.2025.288595 [Epub ahead of print]

The oncogenic ΔNp73 isoform contributes to aggressiveness in acute promyelocytic leukemia

César Alexander Ortiz Rojas[1,2], Diego Antonio Pereira-Martins[1,2,3], Carolina Hassibe Thomé[1], Germano Aguiar Ferreira[1], Thiago Mantelo Bianco[1,4], Isabel Weinhäuser[1,2,3], Ana Silvia Gouvêa[4], Priscila S. Scheucher[4], Cleide Lúcia Araújo Silva[1], Gerwin Huls[3], Abel Bermudez[5], Fernando Garcia[5], Sharon Pitteri[5], Vitor Marcel Faça[1,6], Emanuele Ammatuna[3], Jan Jacob Schuringa[3], Ana Beatriz Glória[7], Katia Borgia Barbosa Pagnano[8], Elenaide Coutinho Nunes[9], Fabiola Traina[1,4], Lorena Lôbo de Figueiredo-Pontes[1,4], Eduardo Magalhães Rego[1,2]

Affiliations: [1]Center for Cell-Based Therapy, University of São Paulo, Ribeirão Preto, Brazil; [2]Laboratório de Investigação Médica (LIM) 31, Hospital das Clínicas HCFMUSP, Faculdade de Medicina, Universidade de São Paulo, São Paulo, Brazil; [3]Department of Hematology, Cancer Research Centre Groningen, University Medical Centre Groningen, University of Groningen, Groningen, The Netherlands; [4]Department of Medical Imaging, Hematology, and Oncology, Ribeirão Preto Medical School, University of São Paulo, Ribeirão Preto, Brazil; [5]Department of Radiology and Canary Center at Stanford for Cancer Early Detection, Stanford University School of Medicine, Stanford, CA 94305, USA [6]Department of Biochemistry and Immunology, Ribeirão Preto Medical School, University of São Paulo, Ribeirão Preto, Brazil; [7]Hematology Division, Federal University of Minas Gerais, Belo Horizonte, Brazil; [8]Hematology and Hemotherapy Center, Centro de Hematologia e Hemoterapia, University of Campinas, Campinas, Brazil; [9]Hematology Division, Federal University of Paraná, Curitiba, Brazil.

Corresponding author information:

Eduardo M Rego (E.M.R.), Hematology Division, Department of Internal Medicine, LIM31, Faculdade de Medicina da Universidade de São Paulo, Av Dr Enéas de Carvalho Aguiar 155, 1o andar, CEP: 05403-000, São Paulo, SP, Brazil. D'Or Institute for Research and Education, Av. República do Líbano, 611 - Ibirapuera, CEP: 04501-000, São Paulo, Brazil. Email: eduardo.rego@fm.usp.br

Acknowledgments

This investigation was supported by Fundação de Amparo à Pesquisa do Estado de São Paulo (FAPESP, Grant #2013/08135-2). C.A.O.R. received a fellowship from FAPESP (Grant #2023/02952-0). D.A.P-M. received a fellowship from FAPESP (Grant #2017/23117-1). I.W. received a fellowship from FAPESP (Grant #2015/09228-0). I.W and D.A.P-M were sponsored by the Abel Tasman Talent Program (ATTP) of the Graduate School of Medical Sciences of the University of Groningen/University Medical Center Groningen (UG/UMCG), The Netherlands.

Author contributions

C.A.O.R., D.A.P-M., E.A., A.B, F.G. and E.M.R. conceived and designed the study, performed experiments, analyzed, and interpreted data, performed the statistical analyses, and drafted the article. C.H.T., G.A.F., T.B., I.W., and C.L.A.S. conceived and designed the study and reviewed the paper. G.H., S.P., V.M.F., S.P., J.J.S., F.T. and L.L.F.P., reviewed the paper. F.T., L.L.F.P., A.S.G., P.S.S., A.B.G., K.P. and E.C.N., provided patient samples and clinical data and reviewed the paper. E.M.R. gave final approval of the submitted version.

Disclosure of conflicts of interest

The authors have no competing financial interests.

Data availability statement

The data generated from this work is open to be shared under request to the authors.

The road to developing effective therapies against acute promyelocytic leukemia (APL) saw a significant turn with the emergence of *all-trans*-retinoic acid (ATRA) and arsenic trioxide (ATO).[1] However, in the context of low- and middle-income countries the access to ATO as frontline therapy is limited,[2] thereby maintaining the ATRA-chemotherapy regimen as the first option, with consequent prognostic implications for APL patients. In this scenario, a deeper understanding of molecular mechanisms of ATRA sensitivity and the identification of biomarkers markers continues to be relevant.

Our group has previously described the association between higher *ΔNp73*/*TAp73* transcripts ratios and the unfavorable treatment outcome in Brazilian patients treated with ATRA+chemotherapy.[3] Both transcripts are encoded by the *TP73* gene, which shares significant sequence homology with *TP53*.[4] Functionally, TAp73 and p53 have similar effects because of their transactivation domains (TAD), that have higher homology. In contrast, ΔNp73 lacks the TAD, and binds to DNA at the same regions of TAp73 and p53 but does not induce gene transcription of their targets. While the role of both isoforms in tumor aggressiveness is well known in solid tumors,[5,6] the functional consequences of ΔNp73 and TAp73 overexpression in leukemias are poorly understood. Here, we confirmed the prognostic role of p73 isoforms in APL patients treated with ATRA + chemotherapy and evaluated the effect of ΔNp73 and TAp73 expression on ATRA and ATO response using *in vitro* and *in vivo* models.

First, we analyzed diagnostic bone marrow (BM) samples of patients (n=98) enrolled in the International Consortium of Acute Promyelocytic Leukemia (IC-APL) from October 2006 through September 2011.[7] For comparison, BM samples from healthy individuals (n=14) without hematological abnormalities were included. Written informed consent was obtained from all patients according to the Declaration of Helsinki (CAAE: 819878.5.1001.5440). When comparing the expression with healthy BM, we found a reduced expression of *TAp73* and a high expression of *ΔNp73* in APL primary blasts (Figure 1A). Subsequently, we evaluated the prognostic significance of both isoforms in APL patients treated with ATRA + chemotherapy. As shown in Figure 1B, we found that higher transcript levels of *ΔNp73* were associated with lower OS rates. The OS rate at 5 years of patients with higher *ΔNp73* expression was 77.8% (95% CI, 68.5%-88.4%) versus 96.6% (95% CI, 90%-100%) in those with expression values below the cut-off. The frequency of early deaths was higher in the group of patients with higher *ΔNp73* expression values (Supplementary Table S1). On the other hand, *TAp73* expression was

not associated with prognosis (Figure 1B) or with any clinical-epidemiological (such as sex and age) or genetic characteristic (data not shown).

To delve into the difference of *TP73* isoforms in APL cells, we induced stable overexpression (OE) of the ΔNp73α or TAp73α isoforms in NB4 (ATRA-sensitive) and NB4-R2 cells (ATRA-resistant) by using a lentivirus system. A tagged GFP was included to express together the p73 isoforms in our strategy. Similar levels of gene expression of two isoforms were observed (Supplementary Figure 1A) in the modified cells. However, at the protein level, the abundance of ΔNp73α was superior to TAp73α in both cell lines (Supplementary Figure 1B), suggesting regulation at protein level. The cells harboring ΔNp73α presented higher proliferation rates compared to their controls, whereas no differences were observed for TAp73α overexpressing cells (Supplementary Figure 1C). We then evaluated whether these isoforms could regulate the apoptosis response, after treatment with ATO (1 μM) or ATO+ATRA (1 μM each). Overall, across the different time-points evaluated we detected minor or non-significative differences in apoptosis induction on NB4 and NB4-R2 cells overexpressing ΔNp73α or TAp73α, when compared to the empty vector control (Supplementary Figure 1D-E). These results contrast with our recent report analyzing primary APL blasts in which ΔNp73 OE was induced. Compared to controls, ΔNp73α OE blasts showed significantly lower rates of apoptosis induced by the *ex vivo* treatment with ATRA, ATO and ATRA+ATO.[8] These results may reflect differences between NB4 cell lines and primary cells, suggesting that the effect of ΔNp73α is more relevant in the latter.

Based on previously published data showing that TAp73 isoform is implicated in cell cycle arrest and apoptosis induced by cellular stress in cell lines of lung carcinoma,[9] we questioned whether increased TAp73α OE would restore the ATO sensitivity in ATO-resistant (ATOr) NB4 cell lines (carrying a PML S214L mutation). These cells were generated by long-term exposure to increasing concentrations of ATO, until cell death was inferior to 10%. TAp73α -OE in ATOr cells resulted in increased ATO-induced apoptosis, both in monotherapy and in combination with ATRA (Supplementary Figure 1F).

Next, we aimed to determine if p73 isoforms could affect the ATRA-induced myeloid differentiation. First, we quantified the expression of CD11b, CD14 and CD15 markers by flow cytometry in ATRA-treated NB4 cells. We found that ΔNp73α prevented the ATRA-induced upregulation of CD11b, CD14, and CD15, suggesting possible disruption of ATRA-induced differentiation (Figure 1C and Supplementary Figure 1G). However, when we evaluated the restoration of PML nuclear bodies and cell morphology after ATRA

exposure, no differences were observed in comparison with control cells, indicating that canonical ATRA effect was not affected (Figure 1D, Supplementary Figure 1H). In this line, p73 isoforms did not impact on ATRA-induced expression of *CEBPA*, *CEBPE*, and *ELANE*, well-known ATRA targets involved in myeloid differentiation (Supplementary Figure 2A). Taking together these results suggest that p73 isoforms do not affect ATRA-induced differentiation. Next, because it was recently described that the BMP4-ΔNp73-NANOG signaling cascade could increase the stem cell-like features of AML cells,[10] we measured the expression of *BMP4* and *NANOG*. We found that these genes were upregulated in ΔNp73α-OE cells, but only during ATRA treatment, with no differences observed in untreated cells (Figure 1E), suggesting a possible role of this signaling axis in the ATRA response. In addition, ATRA treatment led to an increase in ΔNp73α protein levels (Supplementary Figure 2B), indicating that ΔNp73α gains protein stability in the context of ATRA treatment.

To deepen in how p73-dependent pathways could affect APL cells, the total proteomic profile of ΔNp73α- or TAp73-NB4 cells, with or without ATRA exposure, was analyzed. Briefly, 100 µg of protein of each sample was subjected to reduction, alkylation, and overnight tryptic digestion. Then, peptides were purified, dried, and labeled with TMT reagents according to the manufacturer's protocol (Thermo Fisher Scientific). Labeled peptides were separated by nanoflow liquid chromatography and analyzed using an Orbitrap Tribrid Eclipse mass spectrometer (Thermo Fisher Scientific).[11] Protein identification and quantification were performed with MaxQuant, referencing the human proteome (Swiss-Prot, 20,366 entries, 2020).[12] Next, for cellular pathways evaluation, enrichment scores were calculated based on Kolmogorov–Smirnov statistics after applying spearman coefficient as metric for ranking genes and tested for significance (FDR<0.05) using 1000 permutations. As a result, the top upregulation pathways in ΔNp73α-OE NB4 cells were related to the RNA splicing process, whereas these pathways were downregulated when TAp73α was overexpressed (Supplementary Figure 2C). In contrast, this pathway was downregulated during the ATRA treatment independent of the presence of the p73 isoforms (Supplementary Figure 2D). To look for protein interactions and individual proteins altered in different conditions, the proteins differentially abundant in different conditions were evaluated by STRING (https://string-db.org/).[13] As seen in Figure 2, seven clusters of proteins were identified after comparing cells treated with ATRA versus controls. This analysis confirms that p73 isoforms regulate splicing-related proteins (clusters 2 and 3), but also shows that some of the proteins are differently modulated by

p73 isoforms even during ATRA treatment (cluster 2 and 3). Additionally, motor proteins (like DYNC1H1), clathrin binding elements (CLTCL1, CLTC and COPG1), nucleotides and fatty acids metabolism enzymes (FASN and CAD), and proteins related to ion transporter (ATP1A1, ATP2A2, VDAC3 and SLC25A3) were downregulated in ΔNp73α-OE cells while up-regulated in TAp73-OE cells. Finally, we found that NAP1L1 and ANP32E (cluster 5), proteins involved in chromatin accessibility during embryonic stem cell differentiation[14] by interaction with sox motifs,[14,15] are upregulated in ΔNp73α-OE cells only during the ATRA treatment. This last finding is in line with the upregulation of *NANOG* observed in ATRA-treated ΔNp73α-OE cells. This data suggests that, although ΔNp73α does not block the core molecular differentiation process induced by ATRA, it represses surface markers related to mature leukocytes and upregulates stemness-associated factors upon ATRA exposure. This suggests that ΔNp73α could maintain a degree of stemness even under differentiation pressure.

To validate our data, we evaluated p73 isoforms in an APL transgenic murine model. A total of 1×10^4 ΔNp73α or TAp73α OE GFP^+ murine APL blasts ($CD117^+Gr1^{dim}$, Figure 3A) obtained from leukemic hCG-PML::RARA mice were transplanted intravenously to 8 weeks old NOD/SCID gamma (NSG) mice. As shown in Figure 3B, after 14 days of transplant, we divided the animals into three treatment groups: ATRA, ATRA+ATO and control groups. Males and females were used in similar proportions in all groups. Then, after 21 days of treatment, spleen and bone marrow tissues were analyzed by flow cytometry to assess leukemic burden by measuring GFP^+ cell content (Figure 3B). All procedures were performed under pathogen-free conditions and approved by the Animal Ethics Committee of the University of São Paulo (protocol #097/2018). As a result, we found a persistence of leukemic cells in bone marrow and spleen after the ATRA treatment in animals transplanted with ΔNp73α overexpressing blasts (Figure 3C-D). In contrast, ATRA drastically reduced the leukemic burden in blasts overexpressing TAp73α or control cells. Of note, we observed a similar response to the combination of ATO plus ATRA regardless of which isoform was expressed.

Overall, our results validate the clinical relevance of TP73 isoforms in APL, confirming that high expression of ΔNp73α is associated with lower overall survival and a higher rate of early death. Our in vivo model corroborates that ΔNp73α favors disease persistence following ATRA treatment, conferring a resistance phenotype not observed with the TAp73 isoform. Mechanistically, this persistence is not driven by blocking canonical granulocytic differentiation. Unlike other molecular alterations such as FLT3-

ITD,[16] ΔNp73α prevents neither the restoration of PML nuclear bodies nor morphological differentiation, indicating a mechanism independent of the PML::RARA fusion. However, we observed that ATRA paradoxically stabilizes ΔNp73α, which concur with the promotion of expression of proteins related to stem-like phenotype only under the pressure of ATRA treatment. This suggests that while ATRA triggers differentiation signaling, in APL cases with higher expression of ΔNp73α can activate stemness and alternative splicing programs, allowing cells to survive despite differentiation pressure. These findings highlight the importance of ΔNp73α not only as a prognostic biomarker but also as a key regulator of cellular plasticity.

References

1. Degos L. [History of acute promyelocytic leukemia]. Rev Prat. 2015;65(8):1114-1118.
2. Pereira-Martins DA, Weinhäuser I, Coelho-Silva JL, et al. Acute promyelocytic leukaemia in low-income and middle-income countries: a Brazilian experience. Lancet Haematol. 2024;11(2):e98-e99.
3. Lucena-Araujo AR, Kim HT, Thomé C, et al. High ΔNp73/TAp73 ratio is associated with poor prognosis in acute promyelocytic leukemia. Blood. 2015;126(20):2302-2306.
4. Osterburg C, Dötsch V. Structural diversity of p63 and p73 isoforms. Cell Death Differ. 2022;29(5):921-937.
5. Pastor-Morate D, Amigo-Morán L, Garranzo-Asensio M, et al. ΔNp73 and its effector targets promote colorectal peritoneal carcinosis and predict survival. J Pathol. 2024;263(3):328-337.
6. Garranzo-Asensio M, Rodríguez-Cobos J, San Millán C, et al. In-depth proteomics characterization of ΔNp73 effectors identifies key proteins with diagnostic potential implicated in lymphangiogenesis, vasculogenesis and metastasis in colorectal cancer. Mol Oncol. 2022;16(14):2672-2692.
7. Rego EM, Kim HT, Ruiz-Argüelles GJ, et al. Improving acute promyelocytic leukemia (APL) outcome in developing countries through networking, results of the International Consortium on APL. Blood. 2013;121(11):1935-1943.
8. Pereira-Martins D, Ortiz Rojas CA, Weinhaeuser I, et al. CEBPA-Driven Expression of the Transcriptionally Inactive deltaTP73 Isoform Phenocopies TP53 mutated Poor Risk and Drug-Resistant Acute Myeloid Leukemia. Blood. 2023;142(Supplement 1):839.
9. Marini A, Rotblat B, Sbarrato T, et al. TAp73 contributes to the oxidative stress response by regulating protein synthesis. Proc Natl Acad Sci USA. 2018;115(24):6219-6224.
10. Voeltzel T, Flores-Violante M, Zylbersztejn F, et al. A new signaling cascade linking BMP4, BMPR1A, ΔNp73 and NANOG impacts on stem-like human cell properties and patient outcome. Cell Death Dis. 2018;9(10):1011.
11. Tailor D, Garcia-Marques FJ, Bermudez A, Pitteri SJ, Malhotra SV. Guanylate-binding protein 1 modulates proteasomal machinery in ovarian cancer. iScience. 2023;26(11):108292.
12. Cox J, Mann M. MaxQuant enables high peptide identification rates, individualized p.p.b.-range mass accuracies and proteome-wide protein quantification. Nat Biotechnol. 2008;26(12):1367-1372.
13. Szklarczyk D, Kirsch R, Koutrouli M, et al. The STRING database in 2023: protein-protein association networks and functional enrichment analyses for any sequenced genome of interest. Nucleic Acids Res. 2023;51(D1):D638-D646.
14. Li Z, Gadue P, Chen K, et al. Foxa2 and H2A.Z mediate nucleosome depletion during embryonic stem cell differentiation. Cell. 2012;151(7):1608-1616.
15. Ruff GL, Murphy KE, Smith ZR, Vertino PM, Murphy PJ. Subtype-Independent

ANP32E Reduction During Breast Cancer Progression in Accordance with Chromatin Relaxation. BMC Cancer. 2021;21(1):1342.

16. Esnault C, Rahmé R, Rice KL, et al. FLT3-ITD impedes retinoic acid, but not arsenic, responses in murine acute promyelocytic leukemias. Blood. 2019;133(13):1495-1506.

Figure legends

Figure 1. Expression levels, survival association and effect on ATRA-induced differentiation of *TAp73α* and *ΔNp73α* in acute promyelocytic leukemia. (A) Normalized copy numbers (NCN, #copies of target gene/copies of *ACTB*) of *TAp73* (left) and *ΔNp73* (right) in APL samples and healthy bone marrow. Number of (B) Overall survival (Kaplan-Meier) according to expression levels of *Tap73* (left) and *ΔNp73α* (right). The cutoffs used to establish patients with high and low expression were calculated from overall survival (OS) data by using the receiver operating characteristic (ROC) curve and those were 43.4 and 105.6 for *TAp73* and *ΔNp73*, respectively. (C) Percentage levels of the CD11b marker in ATRA-treated NB4 cells overexpressing p73 isoforms. (D) PML-nuclear bodies restoration evaluated by immunofluorescence microscopy after incubation with the PG-M3 monoclonal antibody in NB4 cells treated with ATRA for 96 h. (E) *BMP4*, and *NANOG* expressions were evaluated in NB4 cells, finding that ΔNp73 modulates positively the BMP4/NANOG axis during the ATRA treatment.

Figure 2. Proteomic profiling and protein-protein interaction networks regulated by p73 isoforms in ATRA-treated NB4 cells. Hierarchical clustering heatmap showing the total proteomic profile of NB4 cells with stable overexpression of TAp73α, ΔNp73α, or empty vector control, treated with either vehicle or ATRA (1 μM) for 48 hours. The color scale represents row-scaled protein abundance (Z-score), with red indicating high expression and blue indicating low expression. Seven distinct protein clusters based on expression patterns are identified by the color bars on the left. Specific proteins involved in chromatin accessibility and stress response, such as NAP1L1, RCN2, and ANP32E, are highlighted with arrows. The diagrams on the right show STRING protein-protein interaction networks derived from selected clusters, illustrating enriched biological processes and functional pathways differentially modulated by p73 isoforms and ATRA.

Figure 3. ΔNp73α reduces blast clearance induced by ATRA in an APL mice model. (A) To evaluate the effect of p73 isoforms in vivo, we transplanted overexpressing ΔNp73α or TAp73α, or control APL blasts (from leukemic hCG-PML-RARA) to NSG mice. After lentiviral infection, we enriched the modified cells by sorting the GFP+ cells, achieving more than 98% of purity. As shown in the figure, the CD117+ cells were the main cell population in the GFP+ fraction. (B) Treatment scheme and groups of animals evaluated

in the experiment. (C-D) Leukemic burden, evaluated by GFP+ cells, in bone marrow and spleen after 21 days of treatment, showing that ΔNp73α reduces the blast-clearance induced by ATRA in comparison with the control group.

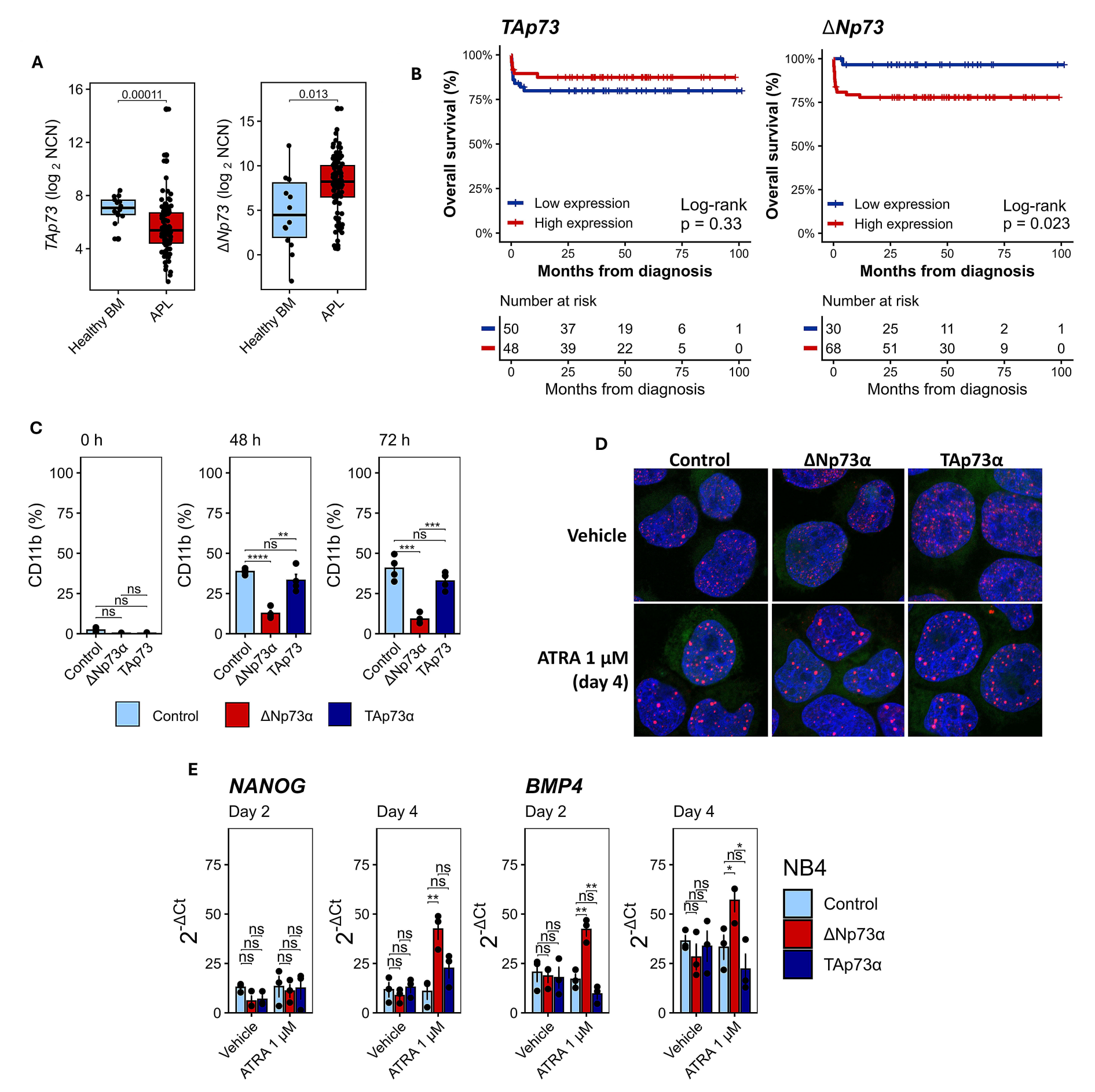
A
TAp73 (log 2 NCN)
ΔNp73 (log 2 NCN)
0.00011
0.013
Healthy BM
APL
B
TAp73
ΔNp73
Overall survival (%)
Low expression
High expression
Log-rank p = 0.33
Log-rank p = 0.023
Months from diagnosis
Number at risk
50 37 19 6 1
48 39 22 5 0
30 25 11 2 1
68 51 30 9 0
C
0 h
48 h
72 h
CD11b (%)
Control
ΔNp73α
TAp73
D
Control
ΔNp73α
TAp73α
Vehicle
ATRA 1 μM (day 4)
E
NANOG
BMP4
Day 2
Day 4
2-ΔCt
Vehicle
ATRA 1 μM
NB4

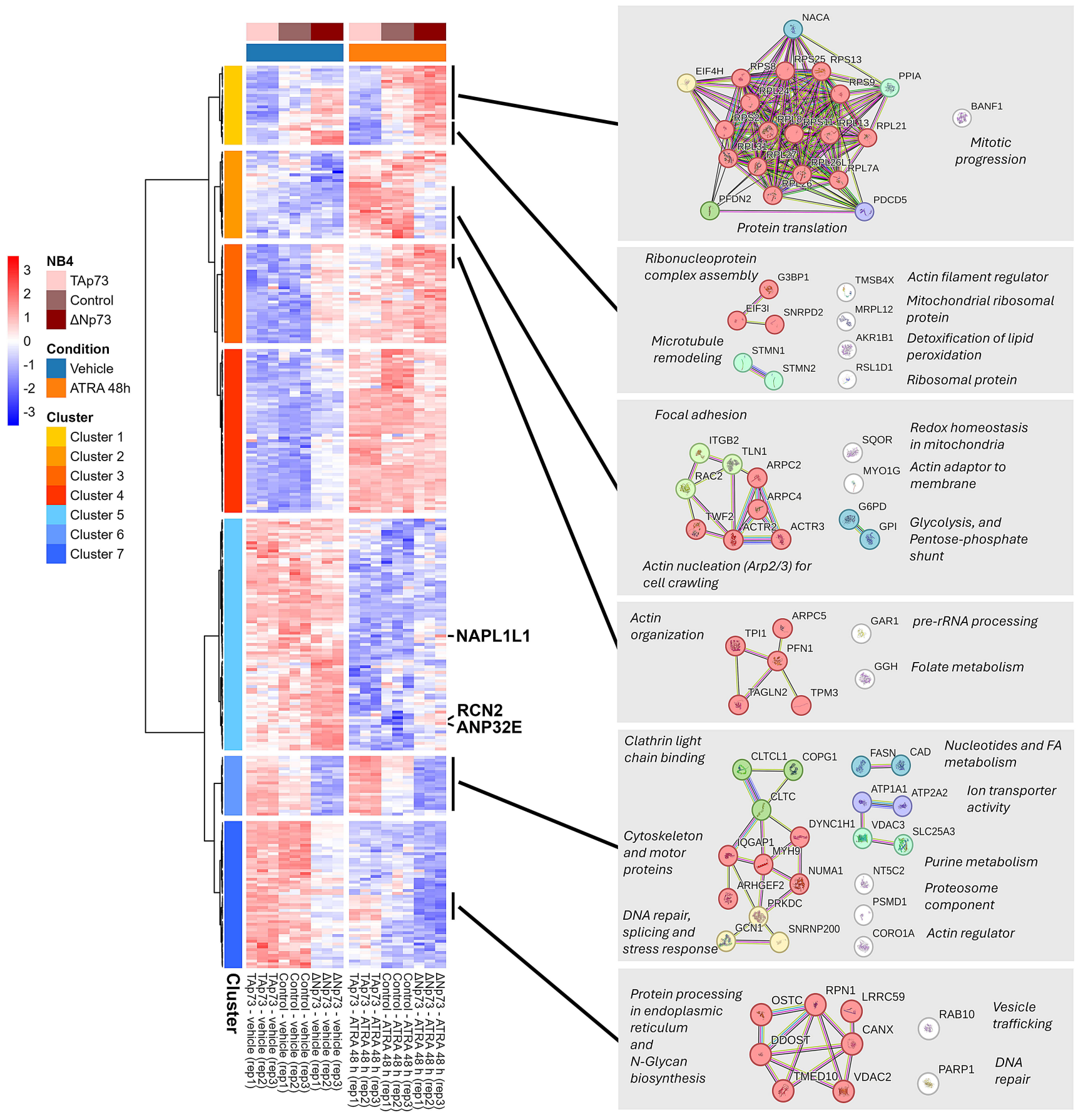
NB4
TAp73
Control
ΔNp73
Condition
Vehicle
ATRA 48h
Cluster
Cluster 1
Cluster 2
Cluster 3
Cluster 4
Cluster 5
Cluster 6
Cluster 7
3
2
1
0
-1
-2
-3
NAPL1L1
RCN2
ANP32E
Cluster
TAp73 - vehicle (rep1)
TAp73 - vehicle (rep2)
TAp73 - vehicle (rep3)
Control - vehicle (rep1)
Control - vehicle (rep2)
Control - vehicle (rep3)
ΔNp73 - vehicle (rep1)
ΔNp73 - vehicle (rep2)
ΔNp73 - vehicle (rep3)
TAp73 - ATRA 48 h (rep1)
TAp73 - ATRA 48 h (rep2)
TAp73 - ATRA 48 h (rep3)
Control - ATRA 48 h (rep1)
Control - ATRA 48 h (rep2)
Control - ATRA 48 h (rep3)
ΔNp73 - ATRA 48 h (rep1)
ΔNp73 - ATRA 48 h (rep2)
ΔNp73 - ATRA 48 h (rep3)
NACA
EIF4H
RPS8
RPS25
RPS13
PPIA
RPS9
RPL24
RPS2
RPL8
RPS11
RPL13
RPL21
RPL34
RPL27
RPL26L1
RPL7A
RPL26
PFDN2
PDCD5
Protein translation
BANF1
Mitotic progression
Ribonucleoprotein complex assembly
G3BP1
EIF3I
SNRPD2
Microtubule remodeling
STMN1
STMN2
TMSB4X
Actin filament regulator
MRPL12
Mitochondrial ribosomal protein
AKR1B1
Detoxification of lipid peroxidation
RSL1D1
Ribosomal protein
Focal adhesion
ITGB2
TLN1
ARPC2
RAC2
ARPC4
TWF2
ACTR2
ACTR3
Actin nucleation (Arp2/3) for cell crawling
SQOR
Redox homeostasis in mitochondria
MYO1G
Actin adaptor to membrane
G6PD
GPI
Glycolysis, and Pentose-phosphate shunt
Actin organization
ARPC5
TPI1
PFN1
TAGLN2
TPM3
GAR1
pre-rRNA processing
GGH
Folate metabolism
Clathrin light chain binding
CLTCL1
COPG1
CLTC
Cytoskeleton and motor proteins
DYNC1H1
IQGAP1
MYH9
NUMA1
ARHGEF2
PRKDC
DNA repair, splicing and stress response
GCN1
SNRNP200
FASN
CAD
Nucleotides and FA metabolism
ATP1A1
ATP2A2
Ion transporter activity
VDAC3
SLC25A3
Purine metabolism
NT5C2
Proteosome component
PSMD1
CORO1A
Actin regulator
Protein processing in endoplasmic reticulum and N-Glycan biosynthesis
OSTC
RPN1
LRRC59
CANX
DDOST
TMED10
VDAC2
RAB10
Vesicle trafficking
PARP1
DNA repair

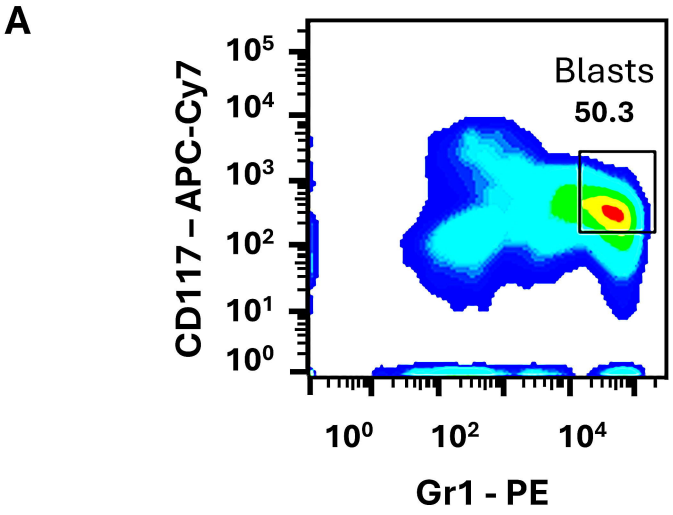

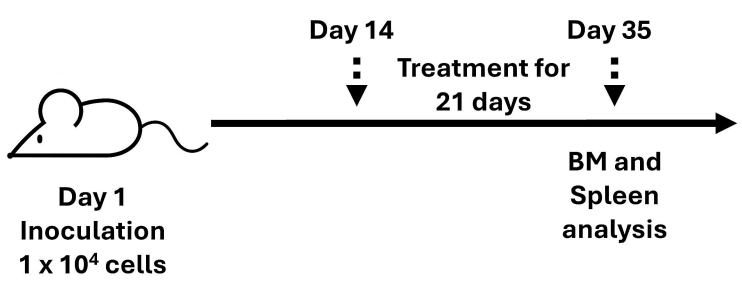

Treatment groups
Group 1: Vehicle
Group 2: ATRA (1.5 mg/Kg/day)
Group 3: ATRA (1.5 mg/Kg /day) + ATO (5 mg/Kg /day)

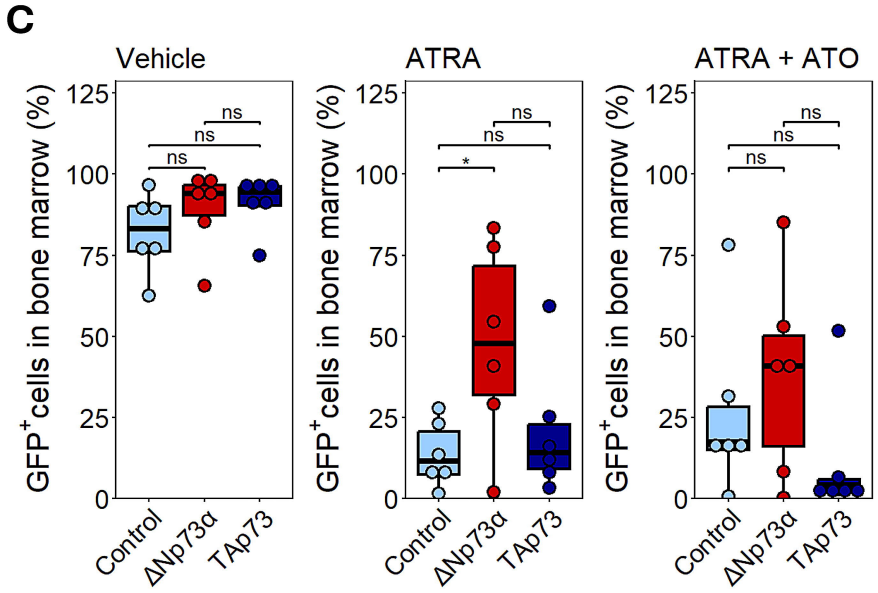

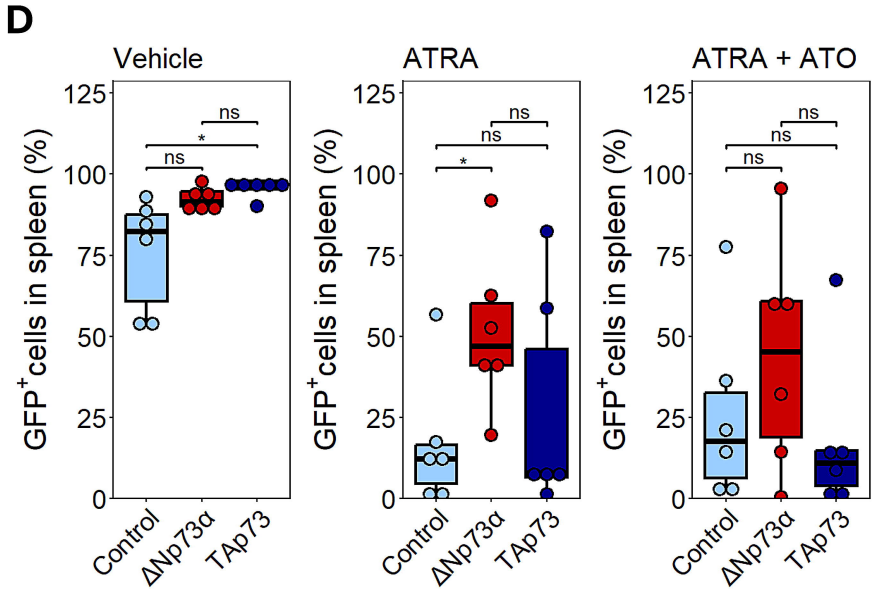

Supplementary Table and Figures

The oncogenic ΔNp73 isoform contributes to aggressiveness in acute promyelocytic leukemia

César Alexander Ortiz Rojas[1,2], Diego Antonio Pereira-Martins[1,2,3], Carolina Hassibe Thomé[1], Germano Aguiar Ferreira[1], Thiago Mantelo Bianco[1,4], Isabel Weinhäuser[1,2,3], Ana Silvia Gouvêa[4], Priscila S. Scheucher[4], Cleide Lúcia Araújo Silva[1], Gerwin Huls[3], Abel Bermudez[5], Fernando Garcia[5], Sharon Pitteri[5], Vitor Marcel Faça[1,6], E. Ammatuna[3], Jan Jacob Schuringa[3], Ana Beatriz Glória[7], Katia Pagnano[8], Elenaide C. Nunes[9], Fabiola Traina[1,4], Lorena Lôbo de Figueiredo Pontes[1,4], Eduardo Magalhães Rego[1,2]

Affiliations: [1]Center for Cell-Based Therapy, University of São Paulo, Ribeirão Preto, Brazil; [2]Laboratório de Investigação Médica (LIM) 31, Hospital das Clínicas HCFMUSP, Faculdade de Medicina, Universidade de São Paulo, São Paulo, Brazil; [3]Department of Hematology, Cancer Research Centre Groningen, University Medical Centre Groningen, University of Groningen, Groningen, The Netherlands; [4]Department of Medical Imaging, Hematology, and Oncology, Ribeirão Preto Medical School, University of São Paulo, Ribeirão Preto, Brazil; [5]Department of Radiology and Canary Center at Stanford for Cancer Early Detection, Stanford University School of Medicine, Stanford, CA 94305, USA [6]Department of Biochemistry and Immunology, Ribeirão Preto Medical School, University of São Paulo, Ribeirão Preto, Brazil; [7]Hematology Division, Federal University of Minas Gerais, Belo Horizonte, Brazil; [8]Hematology and Hemotherapy Center, Centro de Hematologia e Hemoterapia, University of Campinas, Campinas, Brazil; [9]Hematology Division, Federal University of Paraná, Curitiba, Brazil.

Affiliations: [1]Center for Cell-Based Therapy, University of São Paulo, Ribeirão Preto, Brazil; [2]Laboratório de Investigação Médica (LIM) 31, Hospital das Clínicas HCFMUSP, Faculdade de Medicina, Universidade de São Paulo, São Paulo, Brazil; [3]Department of Hematology, Cancer Research Centre Groningen, University Medical Centre Groningen, University of Groningen, Groningen, The Netherlands; [4]Department of Medical Imaging, Hematology, and Oncology, Ribeirão Preto Medical School, University of São Paulo, Ribeirão Preto, Brazil; [5]Department of Radiology and Canary Center at Stanford for Cancer Early Detection, Stanford University School of Medicine, Stanford, CA 94305, USA

[6]Department of Biochemistry and Immunology, Ribeirão Preto Medical School, University of São Paulo, Ribeirão Preto, Brazil.

Corresponding author information:
Eduardo M Rego (E.M.R.), Hematology Division, Department of Internal Medicine, LIM31, Faculdade de Medicina da Universidade de São Paulo, Av Dr Enéas de Carvalho Aguiar 155, 1o andar, CEP: 05403-000, São Paulo, SP, Brazil. D'Or Institute for Research and Education, Av. República do Líbano, 611 - Ibirapuera, CEP: 04501-000, São Paulo, Brazil. Email: eduardo.rego@fm.usp.br

Supplementary Table 1

Characteristics		ΔNp73 expression		p
		Low	High	
Number of patients		30	68	
Gender (%)	female	14 (46.7)	34 (50.0)	0.828
	male	16 (53.3)	34 (50.0)	
Age (median [IQR])		36.6 [27.9, 43.4]	34.88 [26.42, 48.34]	0.829
Classification risk (%)	Favorable	6 (20.0)	9 (13.2)	0.641
	Intermediate	12 (40.0)	32 (47.1)	
	Adverse	12 (40.0)	27 (39.7)	
Break cluster region (%)	bcr1	17 (58.6)	37 (62.7)	0.458
	bcr2	2 (6.9)	1 (1.7)	
	bcr3	10 (34.5)	21 (35.6)	
ECOG (%)	0	22 (75.9)	38 (55.9)	0.355
	1	3 (10.3)	13 (19.1)	
	2	3 (10.3)	10 (14.7)	
	3	1 (3.4)	7 (10.3)	
Fever at diagnosis (%)	No	13 (44.8)	35 (52.2)	0.657
	Yes	16 (55.2)	32 (47.8)	
FLT3-ITD (%)	Detected	2 (9.5)	15 (23.4)	0.219
	Non detected	19 (90.5)	49 (76.6)	
WBC, 10^9/L (median [IQR])		5930 [1737.5, 24450]	6125 [1850, 30187]	0.905
WBC, no. (%), x 10^9/L	≤ 10	18 (60.0)	40 (58.8)	1
	> 10	12 (40.0)	28 (41.2)	
Platelet, 10^9/L (median [IQR])		27200 [15750, 49500]	25500 [14000, 39000]	0.459
Platelet count, no. (%), x 10^9/L	> 50	8 (26.7)	11 (16.2)	0.271
	≤ 50	22 (73.3)	57 (83.8)	
Hb, g/dL (median [IQR])		8.55 [7.65, 9.07]	8.85 [7.35, 10.10]	0.464
Hb, no. (%), g/dL	> 10	4 (13.3)	19 (27.9)	0.131
	≤ 10	26 (86.7)	49 (72.1)	
Creatinine, mg/dL (median [IQR])		0.79 [0.66, 0.92]	0.80 [0.70, 1.00]	0.228
Creatinine, no. (%), mg/dL	≤ 1.4	29 (96.7)	65 (97.0)	1
	> 1.4	1 (3.3)	2 (3.0)	
Albumin, g/dL (median [IQR])		4.40 [3.80, 4.60]	4.00 [3.60, 4.30]	0.026
Albumin, no. (%), g/dL	> 3.5	21 (100.0)	42 (79.2)	0.028
	≤ 3.5	0 (0.0)	11 (20.8)	
Uric acid, mg/dL (median [IQR])		3.70 [2.58, 5.67]	3.80 [3.20, 5.00]	0.544
Uric acid, no. (%), mg/dL	≤ 7	26 (92.9)	64 (98.5)	0.215
	> 7	2 (7.1)	1 (1.5)	
Fibrinogen, mg/dL (median [IQR])		149.5 [88.3, 196.5]	159.5 [100, 233.8]	0.374
Fibrinogen, no. (%), mg/dL	> 170	13 (46.4)	28 (42.4)	0.821
	≤ 170	15 (53.6)	38 (57.6)	
Complete remission (%)	No	1 (3.3)	12 (17.6)	0.06
	Yes	29 (96.7)	56 (82.4)	
FAB subtype (%)	M3	28 (93.3)	65 (95.6)	0.64
	M3v	2 (6.7)	3 (4.4)	
Early mortality (%)	No	30 (100.0)	57 (83.8)	0.017
	Yes	0 (0.0)	11 (16.2)	

*IQR: Interquartile range. Categorical variables were compared with Fisher's exact test while continuous variables with Mann-Whitney test.

Supplementary Figure legends

Supplementary Figure 1. Effect of ΔNp73α and TAp73α on the proliferation and ATO response of NB4 and NB4-R2 cells. (A) Normalized copy numbers (NCN, N copies of target gene/copies of *ACTB*) of OE cells versus controls (transduced with empty vector). (B) Protein abundance of ΔNp73α and TAp73α in OE NB4, NB4-R2, and control cells. The antibodies used to detect ΔNp73α was the pan anti-p73 antibody (Novus biologicals: NB100-56674, 1:1000) and for TAp73 we used an anti-TAp73 (abcam: ab14430; 1:1000). (C) Proliferation assay of transduced APL cells showing higher proliferation index in ΔNp73α OE-NB4 cells. (D-E) Annexin V apoptosis assay after treatment with ATO (D) or ATO+ATRA (E) in OE-NB4 and -NB4-R2, and control cells. (F) Apoptosis assay in NB4 ATOr cells overexpressing TAp73 indicating resensitization to ATO mediated by TAp73. (G) Percentage levels of CD14 and CD15 markers in ATRA-treated NB4 cells overexpressing p73 isoforms. (H) Wright's stain of transduced NB4 cells after 120 h of ATRA-treatment and controls.

Supplementary Figure 2. Evaluation of ATRA-modulated genes and proteome analysis of ATRA-treated NB4 overexpressing ΔNp73α or TAp73α. (A) CEBPA, CEBPE, and ELANE expressions were evaluated during the ATRA-treatment, finding no impact of ΔNp73α or TAp73α. (B) Increased stability of ΔNp73α protein observed during ATRA treatment. (C) Following a proteomic approach, pathway enrichment analysis revealed RNA splicing processes as top differentially modulated between ΔNp73α and TAp73α in NB4 cells. (D). However, these same pathways were uniformly downregulated during ATRA treatment, regardless of p73 isoform overexpression.

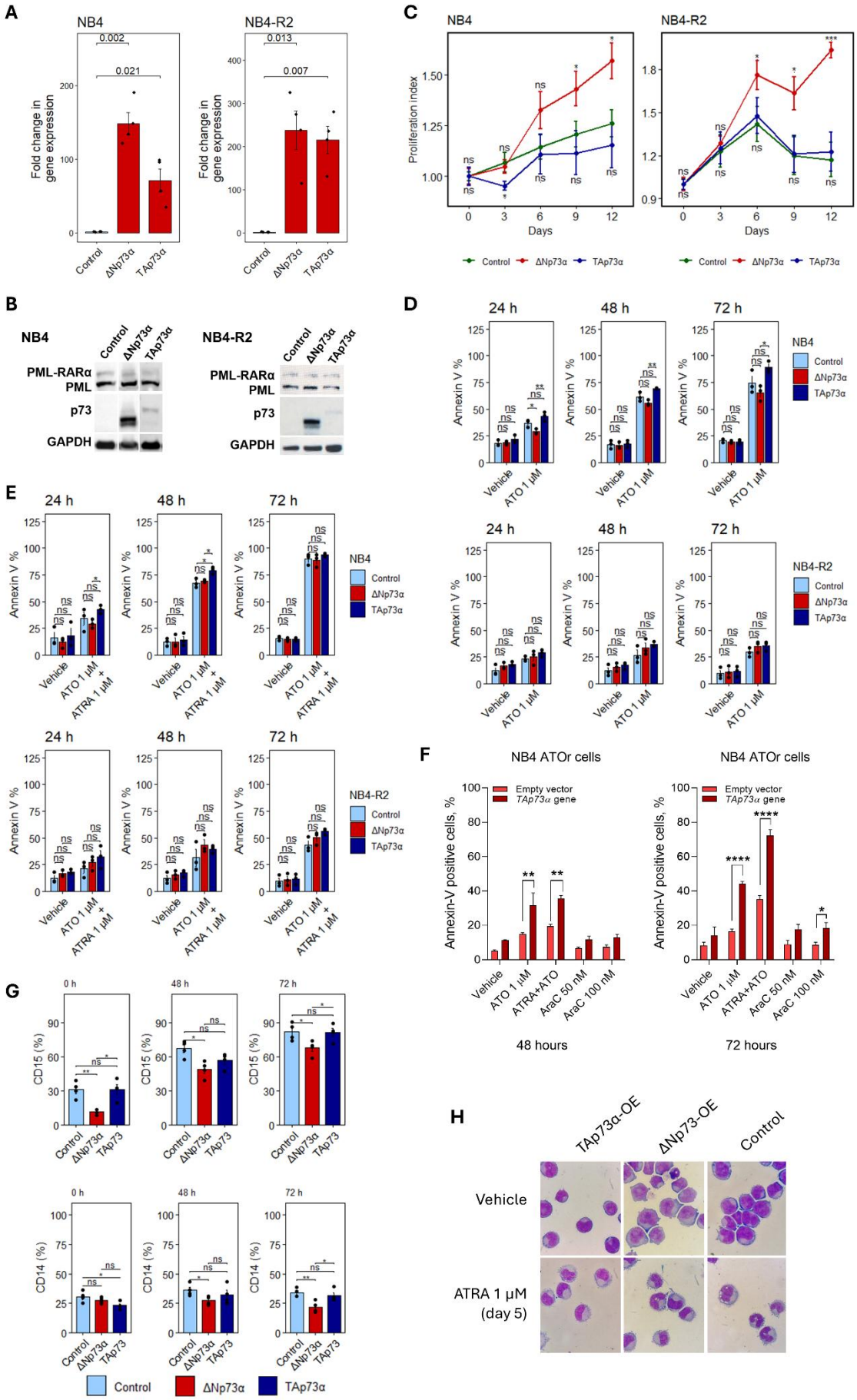
A
NB4
NB4-R2
Fold change in gene expression
0.002
0.021
0.013
0.007
Control
ΔNp73α
TAp73α
B
NB4
NB4-R2
PML-RARα
PML
p73
GAPDH
C
NB4
NB4-R2
Proliferation index
Days
D
24 h
48 h
72 h
Annexin V %
Vehicle
ATO 1 μM
E
ATO 1 μM + ATRA 1 μM
F
NB4 ATOr cells
Empty vector
TAp73α gene
Annexin-V positive cells, %
ATRA+ATO
AraC 50 nM
AraC 100 nM
48 hours
72 hours
G
CD15 (%)
CD14 (%)
TAp73
H
TAp73α-OE
ΔNp73-OE
Control
Vehicle
ATRA 1 μM (day 5)

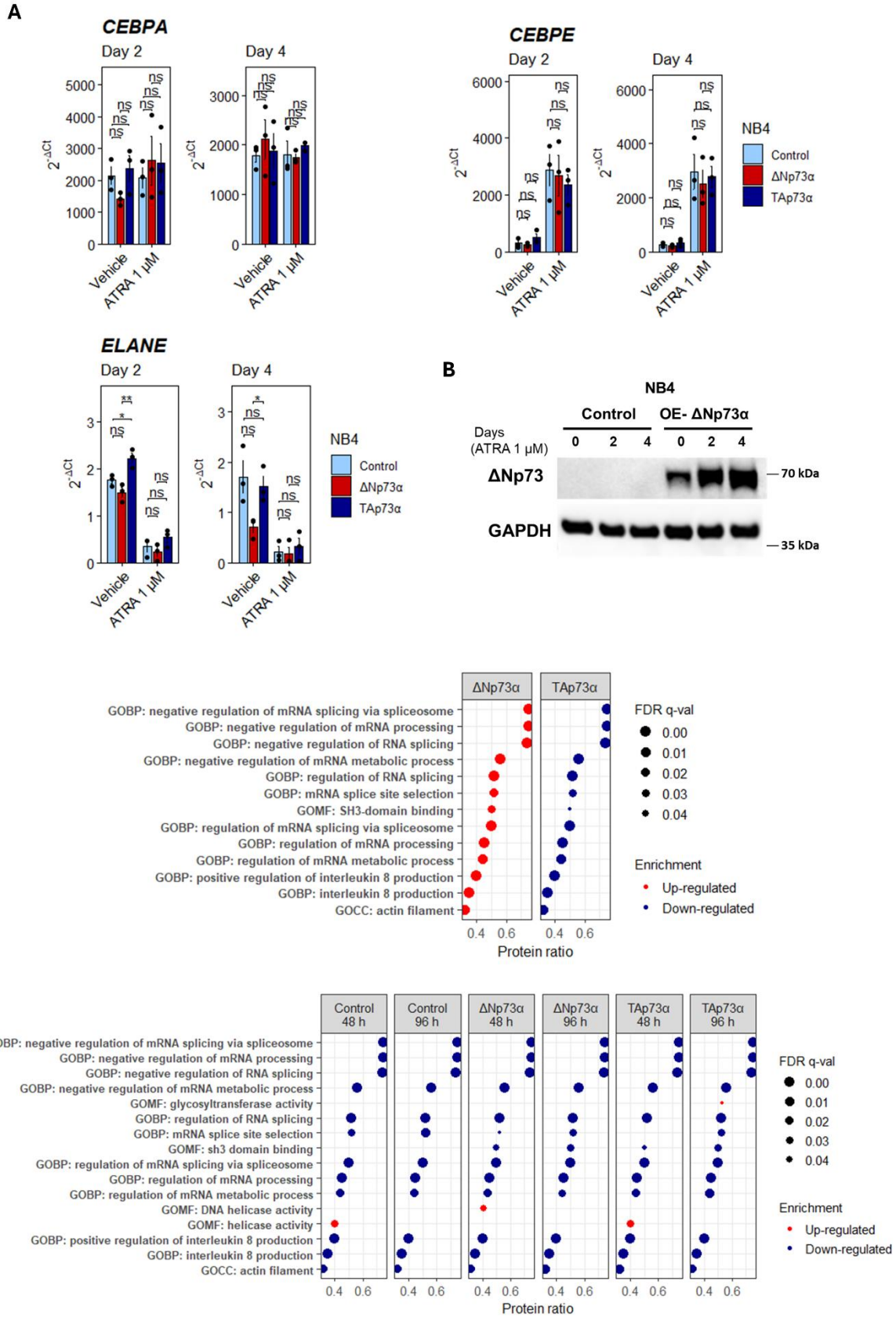
A
CEBPA
Day 2
Day 4
CEBPE
Day 2
Day 4
ELANE
Day 2
Day 4
NB4
Control
ΔNp73α
TAp73α
Vehicle
ATRA 1 μM
B
NB4
Control
OE- ΔNp73α
Days (ATRA 1 μM)
0 2 4 0 2 4
ΔNp73
GAPDH
70 kDa
35 kDa
C
ΔNp73α
TAp73α
GOBP: negative regulation of mRNA splicing via spliceosome
GOBP: negative regulation of mRNA processing
GOBP: negative regulation of RNA splicing
GOBP: negative regulation of mRNA metabolic process
GOBP: regulation of RNA splicing
GOBP: mRNA splice site selection
GOMF: SH3-domain binding
GOBP: regulation of mRNA splicing via spliceosome
GOBP: regulation of mRNA processing
GOBP: regulation of mRNA metabolic process
GOBP: positive regulation of interleukin 8 production
GOBP: interleukin 8 production
GOCC: actin filament
Protein ratio
FDR q-val
0.00
0.01
0.02
0.03
0.04
Enrichment
Up-regulated
Down-regulated
D
Control 48 h
Control 96 h
ΔNp73α 48 h
ΔNp73α 96 h
TAp73α 48 h
TAp73α 96 h
GOBP: negative regulation of mRNA splicing via spliceosome
GOBP: negative regulation of mRNA processing
GOBP: negative regulation of RNA splicing
GOBP: negative regulation of mRNA metabolic process
GOMF: glycosyltransferase activity
GOBP: regulation of RNA splicing
GOBP: mRNA splice site selection
GOMF: sh3 domain binding
GOBP: regulation of mRNA splicing via spliceosome
GOBP: regulation of mRNA processing
GOBP: regulation of mRNA metabolic process
GOMF: DNA helicase activity
GOMF: helicase activity
GOBP: positive regulation of interleukin 8 production
GOBP: interleukin 8 production
GOCC: actin filament
Protein ratio
FDR q-val
0.00
0.01
0.02
0.03
0.04
Enrichment
Up-regulated
Down-regulated